Molecular Pharmacology Fast Forward. Published on May 8, 2018 as DOI: 10.1124/mol.117.111385
This article has not been copyedited and formatted. The final version may differ from this version.

Endoxifen, 4-hydroxytamoxifen and an Estrogenic Derivative Modulate Estrogen Receptor Complex Mediated Apoptosis in Breast Cancer.

Philipp Y. Maximov, Balkees Abderrahman, Sean W. Fanning, Surojeet Sengupta, Ping Fan, Ramona F. Curpan, Daniela Maria Quintana Rincon, Jeffery A. Greenland, Shyamala S. Rajan, Geoffrey L. Greene , V. Craig Jordan.

Department of Breast Medical Oncology, University of Texas, MD Anderson Cancer Center, Houston, TX, USA (PYM, BA, PF, DMQR, JAG, VCJ)

The Ben May Department for Cancer Research, University of Chicago, Chicago, IL, USA (SWF, SSR, GLG)

Department of Oncology, Lombardi Comprehensive Cancer Center, Washington, DC, USA (SS)

Institute of Chemistry, Romanian Academy, Timisoara, Romania (RFC)

Molecular Pharmacology Fast Forward. Published on May 8, 2018 as DOI: 10.1124/mol.117.111385
This article has not been copyedited and formatted. The final version may differ from this version.

Running title: Role of the ERα Complex in Apoptosis in Breast Cancer

Corresponding Author:

V. Craig Jordan, OBE, PhD, DSc, FMedSci

University of Texas, MD Anderson Cancer Center,

Department of Breast Medical Oncology,

1515 Holcombe Blvd., Unit 1354

Houston, Texas 77030

Tel: +1(713)792-2121

E-mail: VCJordan@mdanderson.org

Number of text pages: 28

Number of figures: 8

Number of tables: 0

Number of references: 51

Number of words: Abstract- 196

Introduction- 613

Discussion- 870

List of nonstandard abbreviations: TPE (TriPhenylEthylene), MBC (Metastatic Breast Cancer), ER (Estrogen Receptor), E_2 (17β-estradiol), 4OHT (4-hydroxytamoxifen), Endox (Endoxifen), UPR (Unfolded Protein Response), ChIP (Chromatin Immuno-Precipitation), LBD (Ligand-Binding Domain), LTED (Long-Term Estrogen Deprivation)

Molecular Pharmacology Fast Forward. Published on May 8, 2018 as DOI: 10.1124/mol.117.111385
This article has not been copyedited and formatted. The final version may differ from this version.

Abstract

Estrogen therapy was used to treat advanced breast cancer in postmenopausal women for decades until the introduction of tamoxifen. Resistance to long-term estrogen deprivation (LTED) with tamoxifen and aromatase inhibitors used as a treatment for breast cancer inevitably occurs, but unexpectedly low dose estrogen can cause regression of breast cancer and increase disease free survival in some patients. This therapeutic effect is attributed to estrogen-induced apoptosis in LTED breast cancer. Here we describe modulation of the estrogen receptor liganded with antiestrogens (endoxifen, 4-hydroxytamoxifen) and an estrogenic triphenylethylene (TPE) EthoxyTPE (EtOXTPE) on estrogen-induced apoptosis in LTED breast cancer cells. Our results show that the angular TPE estrogen (EtOXTPE) is able to induce the ER-mediated apoptosis only at a later time compared to planar estradiol in these cells. Using RT-PCR, ChIP, Western blotting, molecular modelling and X-ray crystallography techniques we report novel conformations of the ER complex with an angular estrogen EtOXTPE and endoxifen. We propose that alteration of the conformation of the ER complexes, with changes in coactivator binding, governs estrogen-induced apoptosis through the PERK sensor system to trigger an Unfolded Protein Response (UPR).

Molecular Pharmacology Fast Forward. Published on May 8, 2018 as DOI: 10.1124/mol.117.111385
This article has not been copyedited and formatted. The final version may differ from this version.

Introduction

High dose synthetic estrogen therapy was the first successful chemical treatment for any cancer (Haddow et al., 1944). Estrogen was used clinically to treat metastatic breast cancer (MBC) for 30 years prior to the successful introduction of the antiestrogen tamoxifen (Jordan, 2003). Tamoxifen is a structural derivative of the synthetic estrogen triphenylethylene. During the time before tamoxifen, clinical rules were defined for the successful application of high dose estrogen treatment. Therapy was only effective in 30% of MBC and only if applied more than 5 years past menopause (Haddow, 1970). Mechanisms were unknown.

The advantage of tamoxifen compared to high dose estrogen to treat MBC was not an increase in response rate, but a lower incidence of side effects (Cole et al., 1971; Ingle et al., 1981). Targeting tamoxifen to patients with Estrogen Receptor (ER) positive breast cancer, and the safety of the medicine, permitted implementation of translational research (Jordan, 2008, 2014b) to establish the value of tamoxifen as a long-term adjuvant therapy (EBCTCG, 1998). The proposition in the 1970's (Jordan and Allen, 1980; Jordan et al., 1979) that longer adjuvant therapy would be superior to shorter therapy also demanded an investigation of acquired resistance to long-term tamoxifen treatment in breast cancer. Nothing was known.

Acquired resistance to tamoxifen is unique. Initially, laboratory models *in vivo* demonstrated that tamoxifen actually stimulated tumor growth within 1-2 years (Gottardis and Jordan, 1988; Gottardis et al., 1989b). Nevertheless, low dose estrogen also stimulated tumor growth. Mechanisms have subsequently been deciphered using breast cancer cell models *in vitro* (Fan et al., 2014a; Fan et al., 2014b; Fan et al., 2014c). A new steroidal pure antiestrogen was subsequently developed following proof of efficacy *in vivo,* to prevent tumor growth in tumors with acquired resistance (Gottardis et al., 1989a). Fulvestrant is now approved for the first line

Molecular Pharmacology Fast Forward. Published on May 8, 2018 as DOI: 10.1124/mol.117.111385
This article has not been copyedited and formatted. The final version may differ from this version.

and second line treatment of MBC (Howell et al., 2002; Moscetti et al., 2017; Osborne et al., 2002).

It therefore came as some surprise to find that low dose estrogen therapy triggered breast tumor regression following the development of acquired resistance to tamoxifen treatment for 5 years (Yao et al., 2000). This experimental model mimics the 5 years of adjuvant tamoxifen therapy that was the standard of care at the time. The rules described by Haddow (Haddow, 1970) applied to adjuvant tamoxifen therapy: 5 years of estrogen deprivation in ER-positive breast cancer is necessary to sensitize selected cell populations to undergo estrogen-induced apoptosis (Jordan, 2015). This created a general principle of ER positive breast cancer cell biology. Most importantly, low dose estrogen salvage therapy is effective in producing a 30% clinical benefit rate in patients failing long-term adjuvant therapy with aromatase inhibitors (Ellis et al., 2009). Indeed, the science of estrogen-induced apoptosis has also been linked to the antitumor effects of estrogen therapy alone in the Women's Health Initiative (Abderrahman and Jordan, 2016) and responsible for the "carry over effect" that maintains patients recurrence free after adjuvant therapy is terminated at 5 years (Jordan, 2014a).

The clinical significance of estrogen-induced apoptosis requires an understanding of molecular mechanisms to decipher appropriate applications for clinical care. We address the modulation of estrogen-induced apoptosis using estrogens of different shapes and related synthetic non-steroidal antiestrogens.

Haddow documented (Haddow et al., 1944) antitumor activity with both planar synthetic estrogens (diethylestibestrol (DES)) and angular estrogens (triphenylethylenes (TPEs)). In recent years, these synthetic estrogens were classified based on the resulting ER complex to activate or block an estrogen responsive gene. Class I are planar estrogens and class II are angular estrogens

Molecular Pharmacology Fast Forward. Published on May 8, 2018 as DOI: 10.1124/mol.117.111385
This article has not been copyedited and formatted. The final version may differ from this version.

(Jordan et al., 2001), based on their estrogenic or antiestrogenic activity at the transforming growth factor α gene (TGFα). One explanation for the TPE estrogens having early antiestrogenic actions on estradiol-induced apoptosis (Maximov et al., 2011) was that the class II estrogen complex initially induces an antiestrogenic ER:class II estrogen complex (Obiorah et al., 2014), which then evolves to an estrogenic ER:class I complex to trigger apoptosis (Obiorah et al., 2014; Obiorah and Jordan, 2014).

Here we address the hypothesis using X-ray crystallography of a novel type II estrogen known as ethoxytriphenylethylene (EtOXTPE) (Maximov et al., 2011; Maximov et al., 2010) and compare and contrast the ER conformation with the TPE antiestrogen endoxifen, which is the major biologically active secondary metabolite of tamoxifen. The biology of these ER complexes to modulate estrogen-induced apoptosis now opens up new opportunities to examine the elasticity of Unfolded Protein Response (UPR) to trigger or block apoptosis through the PERK sensor in long-term estrogen deprived (LTED) breast cancer cells lines.

Materials and Methods

Cell Culture and Reagents. The test compound was synthesized and the details of the synthesis have been reported previously (Maximov et al., 2010). The 17β-estradiol (E_2) and 4-hydroxytamoxifen (4OHT) were acquired from Sigma-Aldrich (St. Louis, MO). Endoxifen (Z-isomer) was purchased from Santa Crus Biotechnology (Santa Cruz, CA). The ER positive and long-term estrogen-deprived (LTED) breast cancer cells MCF7:5C were derived from MCF7 cells as reported previously (Jiang et al., 1992; Lewis et al., 2005b). MCF7:5C cells were maintained in phenol-red free RPMI 1610 media containing 10% charcoal dextran treated FBS, 6 ng/ml bovine insulin, L-glutamine, penicillin and streptomycin and were incubated at 37ºC with 5% CO_2. The cells were treated with indicated compounds for specified time and then harvested.

Molecular Pharmacology Fast Forward. Published on May 8, 2018 as DOI: 10.1124/mol.117.111385
This article has not been copyedited and formatted. The final version may differ from this version.

Growth Assays. For a 7 day growth assay 10,000 of MCF7:5C cells and 5,000 MCF7:5C cells for 14 day assays were plated in each well of 24 well plates and then treated the next day with specific concentrations of indicated compounds. The assay was carried out as described previously (Maximov et al., 2011; Maximov et al., 2014) using a fluorescent DNA quantitation kit purchased from Bio-Rad (Helcules, CA) with sonication of samples after harvesting in isotonic buffer. All growth assays were performed in triplicate, the results represent the average of all replicates, the error bars represent the standard deviation in each treatment. One-way ANOVA was used with a follow up Tukey's test to determine the statistical significance of the treatments.

Immunoblotting. The MCF-7:5C cells were seeded on 5cm Petri dishes at a density of 2 million cells per plate and were incubated overnight. The cells were treated for specified times with the indicated compounds. Protein isolation and immunoblotting were performed as previously described (Maximov et al., 2014). The primary antibodies used were anti-ERα clone G-20 (Santa Cruz Biotechnology, Santa Cruz, CA), anti-eIF2α (9722) and anti-peIF2α (D9G8) (Santa Cruz Biotechnology, Santa Cruz, CA) and with goat anti-β-actin antibodies (Santa Cruz Biotechnology, Santa Cruz, CA) diluted in 5% dry milk in TBS-T blocking buffer at ratios recommended by the supplier at 4°C. All secondary antibodies were HRP linked (Santa Cruz Biotechnology, Santa Cruz, CA). The signals were visualized by enhanced chemiluminescence (ECL). All immunoblots were performed in three replicates, data presented represents one the biological replicates. Analysis was validated by densitometry using Image J (NIH) and the densitometry data is presented in supplemental tables S1, S2 and S3.

Chromatin Immuno-precipitation (ChIP) Assay. ChIP was performed as described previously (Obiorah et al., 2014; Sengupta et al., 2010) with minor modifications. The DNA

Molecular Pharmacology Fast Forward. Published on May 8, 2018 as DOI: 10.1124/mol.117.111385
This article has not been copyedited and formatted. The final version may differ from this version.

fragments were purified using Qiaquick PCR purification kit (Qiagen, Germantown, MD). Two microliters of eluted DNA was used for real-time PCR analysis. The primer sequences used are as follows: TFF1 Promoter: 5'TGGGCTTCATGAGCTCCTTC3' (forward); 5'TTCATAGTGAGAGATGGCCGG3' (reverse); The data is expressed as percent input of starting chromatin material after subtracting the percent input pull down of the negative control (normal rabbit IgG). The assay was performed in triplicate, the error bars represent the standard deviation in each treatment. One-way ANOVA was used with a follow up Tukey's test to determine the statistical significance of the treatments.

Annexin V staining. MCF-7:5C cells were seeded at 300,000 cells per 10cm Petri dishes and were treated the next day with test compounds. Cells were treated with test compounds for 6 days, and for 3 days with 1nM E_2. Cells were harvested by aspirating media and washing cells with warm PBS twice and subsequently treated with accutase solution (Life Technologies, Grand Island, NY) for 4 minutes at 37˚C. Cells were then harvested by pipetting after addition of PBS and then transferred to centrifuge tubes and precipitated. Cells were put on ice afterwards and were stained using FITC Annexin V Apoptosis Detection kit I (BD Pharmingen, San Diego, CA) according to the manufacturer's instructions. The assay was performed in triplicate, data represents the average of the biological replicates, the error bars represent the standard deviation in each treatment. One-way ANOVA was used with a follow up Tukey's test to determine the statistical significance of the treatments.

Real-Time PCR. MCF-7:5C cells, depending on the duration of treatment, were seeded at the density of 100,000-300,000 per well into 6-well plates. Cells were treated the next day with test compounds for specified time-points. RNA isolation, cDNA synthesis and RT-PCR were performed as previously described (Obiorah et al., 2014). Primers sequences that were used

Molecular Pharmacology Fast Forward. Published on May 8, 2018 as DOI: 10.1124/mol.117.111385
This article has not been copyedited and formatted. The final version may differ from this version.

for human TFF1 cDNA amplification are: 5'-CATCGACGTCCCTCCAGAAGA-3' sense, and 5'-CTCTGGGACTAATCACCGTGCTG-3' anti-sense; human GREB1 gene: 5'-CAAAGAATAACCTGTTGGCCCTGC-3'sense,5'-GACATGCCTGCGCTCTCATACTTA-3' anti-sense; human BCL2L11 gene: 5'-TCGGACTGAGAAACGCAAG-3' sense, 5'-CTCGGTCACACTCAGAACTTAC-3' anti-sense; human TP63 gene: 5'-TTCGGACAGTACAAAGAACGG-3' sense, 5'-GCATTTCATAAGTCTCACGGC-3' anti-sense; human HMOX1 gene: 5'- TCAGGCAGAGGGTGATAGAAG-3' sense, 5'-TTGGTGTCATGGGTCAGC-3' anti-sense; human TNFα gene: 5'-ACTTTGGAGTGATCGGCC-3' sense, 5'-GCTTGAGGGTTTGCTACAAC-3' anti-sense; the reference gene RPLP0: 5'-GTGTTCGACAATGGCAGCAT-3' sense, 5'-GACACCCTCCAGGAAGCGA-3' anti-sense. All primers were obtained from Integrated DNA Technologies Inc. (IDT, Coralville, IA, USA). All treatments were performed in triplicate, data represents average of the replicates, the error bars represent the standard deviation in each treatment. One-way ANOVA was used with a follow up Tukey's test to determine the statistical significance of the treatments.

X-ray crystallography. ERα ligand-binding domain (LBD) was incubated with a mixture of both cis and trans-EtOXTPE isomers prior to crystallization. Separation of geometric isomers was not undertaken. Inclusion of the glucocorticoid receptor interacting protein 1 peptide (GRIP) was necessary to obtain diffraction quality crystals as was the use of Y537S mutation (Nettles et al., 2008). This mutation favors the agonist state of the receptor by forming a hydrogen bond with D351. Sitting drop was used for this crystallization. Clear rectangular crystals were observed after 1 week in 0.15 M KBr, 30% PEG MME 2,000, Tris pH 8.3. Paratone-N was used as the cryo-protectant. The structure was solved to 2.10 Å using molecular

Molecular Pharmacology Fast Forward. Published on May 8, 2018 as DOI: 10.1124/mol.117.111385
This article has not been copyedited and formatted. The final version may differ from this version.

replacement (1GWR was used as the starting model) and one dimer was observed in the asymmetric unit and all EtOXTPE molecules are well ordered in the hormone-binding pocket. Only the trans-isomer of EtOXTPE was present. Coordinates have been deposited in the PDB under accession code 5T1Z. For estradiol complex, ERα LBD Y537S was incubated with 1 mM ligand and 2 mM GRIP peptide overnight at 4°C. Hanging drop vapor diffusion with a Hampton VDX plate was used for crystallization. Clear rectangular crystals were observed after 2 days in 20% PEG 3,350, 100 mM $MgCl_2$, Tris pH 8.0. Paratone-N was used as the cryo-protectant. The structure was solved to 1.65 Å with one dimer in the ASU by molecular replacement with 1GWR as the input model. All estradiol ligands are resolved in the hormone binding pocket. Coordinates were deposited in the PDB under accession code 6CBZ.

An ERα LBD construct with mutations C381S, C417S, C530S, and L536S was used to obtain co-crystal structures with endoxifen or 4OHT. Protein was expressed and purified as previously described (Fanning et al., 2016). Protein was incubated with 2 mM ligand at 4°C overnight prior to crystallization. Hanging drop at room temperature was used for these crystallizations. Clear hexagonal crystals were observed for the endoxifen co-crystals in Tris pH 8.0, 2 mM $MgCl_2$, and 25% PEG 8,000 after 5 days. For the 4OHT co-crystal structure clear hexagonal crystals were observed after 1 week in Tris pH 6.5, 2 mM $MgCl_2$, and 30% PEG 8,000. All 4OHT ligands are resolved in the hormone binding pocket.The endoxifen structure was solved with molecular replacement (using 5ACC as a starting model) to 1.65 Å with 1 dimer in the ASU. The 4OHT structure was solved by molecular replacement (with 5ACC as the starting model) to 1.80 Å with 2 dimers in the ASU. All endoxifen ligands are resolved in the hormone binding pocket. Both structures were deposited in the PBD with accession codes 5W9C for the 4OHT structure and 5W9D for the endoxifen structure.

Molecular Pharmacology Fast Forward. Published on May 8, 2018 as DOI: 10.1124/mol.117.111385
This article has not been copyedited and formatted. The final version may differ from this version.

While structures of ERα LBD with E_2 or 4OHT have been published, they have not been published using the same construct that we were using for the EtOXTPE or endoxifen (with the 537S mutation for EtOXTPE or 381S, 417S, 530S for the endoxifen). Obtaining these structures enabled a more appropriate comparison between the ligands within the hormone binding pocket. Furthermore, the previously published ER:4OHT structure (PDB:3ERT) possesses a crystal contact just after helix 11 that perturbs the loop connecting helices 11 and 12 and appears to alter how H12 sits in the AF2 cleft. Our structure does not have this crystal contact. Therefore, to properly compare endoxifen and 4OHT it was especially important to obtain this new 4OHT structure. The omit maps are shown in the supplemental figure S1.

Results

Effect of non-planar estrogen EtOXTPE alone on MCF-7:5C cells. To assess the activity of the test compounds on the viability of the MCF-7:5C cells (Fig. 1) we have employed the proliferation assay as described in the Materials and Methods section. Following the increases in DNA levels at low concentrations (Fig. 2A), E_2 started to induce apoptosis in cells at a concentration of 10^{-11} M, reducing the amount of viable cells in the wells by 60% after 7 days of treatment (Fig. 2A) ($p< 0.05$ vs. vehicle control). At a concentration of 10^{-10} M E_2 inhibited cell growth further by more than 90% (Fig. 2A) after 1 week of treatment. All other test compounds were used within a 10^{-12} -10^{-6} M concentration range. Compound EtOXTPE produced partial agonist activity inhibiting cell growth on average by 30% at the highest concentration of 10^{-6} M (Fig. 2A) after one week of treatment. Antiestrogen endoxifen produced no apoptotic activity with any statistically significant differences at any concentrations tested (Fig. 2A).

Molecular Pharmacology Fast Forward. Published on May 8, 2018 as DOI: 10.1124/mol.117.111385
This article has not been copyedited and formatted. The final version may differ from this version.

Effect of non-planar estrogen EtOXTPE in combination with 1nM E_2 on MCF7:5C cells. To assess the antiestrogenic properties of the test compounds to block E_2-induced apoptosis, MCF-7:5C cells were treated with the compounds in combination with 1 nM E_2 for 7 days. The results of the DNA quantification show that endoxifen completely inhibits 1 nM E_2-induced apoptosis in the 10^{-7}- 10^{-6} M range with no statistical significance between the DNA values at these concentrations and vehicle control ($p > 0.05$) (Fig. 2B). Compound EtOXTPE has only partial antiestrogenic properties inhibiting 1 nM E_2 according to its intrinsic activity alone at 10-6 M, and do not completely block E_2 action ($p<0.05$ compared to Vehicle control) (Fig. 2B).

Effect of non-planar estrogen EtOXTPE on MCF-7:5C cells after an extended treatment. To assess the activity of the test compounds of the cellular viability alone after an extended treatment we performed the same treatments as described above for 14 days. As a result of longer treatment DNA quantification assay has shown that the non-planar estrogen is able to induce apoptosis in MCF-7:5C cells. Compound EtOXTPE is able to reduce the amount of cells by more than 90% starting at a 10^{-7} M concentration (Fig. 2C) ($p< 0.05$) with an IC_{50} of approximately $2x10^{-9}$ M (Fig. 2C). Antiestrogen endoxifen is completely inactive alone and is not able to produce any reduction of cells at any of the concentration points (Fig. 2C).

Reversal of non-planar estrogen EtOXTPE effects by an antiestrogen in MCF-7:5C cells. To test the possibility of reversal of the proapoptotic actions of the non-planar estrogen EtOXTPE we treated MCF-7:5C cells with the compound for various durations (Fig. 2D) after which antiestrogen 4-hydroxytamoxifen (4OHT) was added at the concentration of 10^{-6} M. The treatments with E_2, EtOXTPE and 4OHT alone were used as controls. The cells were harvested for DNA fluorescent quantification assay as described in the Online Methods section after a total of 14 days of treatment. The results show that the test compound EtOXTPE is able to induce

Molecular Pharmacology Fast Forward. Published on May 8, 2018 as DOI: 10.1124/mol.117.111385
This article has not been copyedited and formatted. The final version may differ from this version.

apoptosis in the cells at 10^{-6} M concentration after 14 days of treatment alone (Fig. 2D) by more than 90% compared to the vehicle control ($p< 0.05$), which is consistent with the dose-response curves with the same compound for equal duration of treatment (Fig. 2D). Addition of 4OHT at an equimolar concentration at early time points almost completely revered the apoptotic actions of EtOXTPE after 1 and 2 days of treatment (Fig. 2D). However, after 4 days of treatment with EtOXTPE, 4OHT was able to reverse apoptotic actions of the estrogen only by 50% of vehicle control (Fig. 2D). After 5 days of treatment with EtOXTPE, 4OHT was able to consistently reverse apoptotic action of the compound by 30% on average throughout the remaining days of treatment in the experiment (Fig. 2D). This result is consistent with previously observed result with another TPE called bisphenol TPE (Obiorah and Jordan, 2014). Compared to planar E_2, both EtOXTPE and biphenolTPE (Obiorah and Jordan, 2014)induce apoptosis consistently in MCF-7:5C cells later than E_2 (Obiorah and Jordan, 2014).

The apoptotic effect of non-planar estrogen EtOXTPE on MCF-7:5C cells is delayed. Cells undergo visual morphologic changes during treatment with EtOXTPE at a delayed rate compared to E_2 (Fig. 3). Results of Annexin V staining demonstrate that EtOXTPE is able to induce positive Annexin V staining after 6 days of treatment compared to vehicle control ($p< 0.05$) (Fig. 4A), whereas, endoxifen did not produce statistically significant change Annexin V staining compared to vehicle control (Fig. 4A) or any morphologic changes (Fig. 3). Besides the positive Annexin V staining results with the test compound, non-planar estrogen is also able to induce activation of the proapaptotic genes, such as TNFα and BCL2L11 in MCF-7:5C cells after 120 hours of treatment compared to the vehicle control ($p< 0.05$) (Fig. 4B & C). All these data indicate that the non-planar estrogen reduces the number of viable cells in the growth assay due to apoptosis and is delayed compared to E_2. To assess the role of PERK

Molecular Pharmacology Fast Forward. Published on May 8, 2018 as DOI: 10.1124/mol.117.111385
This article has not been copyedited and formatted. The final version may differ from this version.

signaling in EtOXTPE-induced apoptosis, we performed Annexin V staining of the treated MCF-7:5C cells with the compound alone and in combination with PERK inhibitor GSK2606414 (Fig. 4D). We show that the inhibition of PERK with a selective inhibitor completely abrogates the EtOXTPE-induced apoptosis when compared with the vehicle control or to the PERK inhibitor alone treatment (Fig. 4D) ($p > 0.05$ in both cases), which is consistent with previously published data on E2-induced apoptosis in the same cell line (Fan et al., 2013).

Activation of estrogen-regulated genes by non-planar estrogen EtOXTPE. To test the impact of the test compounds on the transcription of the some of the estrogen-regulated genes in MCF-7:5C cells, we have treated cells with the test compounds at 10^{-6} M concentration for 24 hours and have used qRT-PCR as described in the Materials and Methods section. The results of experiments show that 1nM E_2 is able to induce mRNA production of TFF1 and GREB1 genes compared to vehicle control ($p < 0.05$) (Fig. 5A and B). Treatment with test compound EtOXTPE produced mRNA production in both TFF1 and GREB1 genes when compared to vehicle controls ($p < 0.05$), but only partially compared to E_2 treatment ($p < 0.05$) at 24 hours (Fig. 5A and B).

Delayed effect on the regulation of ERα mRNA and protein by non-planar estrogen EtOXTPE in MCF-7:5C cells. To assess the regulation of ERα protein and mRNA levels we employed immunoblotting and qRT-PCR. Results of immunoblotting show that E_2 can down regulate ERα protein level considerably as early as 12 hours of treatment with subsequent down regulation maintained (Fig. 6A). Interestingly, non-planar estrogen EtOXTPE can down regulate ERα protein levels to levels comparable with E_2 only after 48 hours of treatment (Fig. 6A). Antiestrogens endoxifen did downregulate the levels of ERα protein compared to vehicle control but equivalently to the 4OHT treatment (Fig. 6A). Interestingly, 1μM 4OHT can reverse the effect of 100nM EtOXTPE down regulation of ERα protein after 24 hours of treatment (Fig. 6B).

Molecular Pharmacology Fast Forward. Published on May 8, 2018 as DOI: 10.1124/mol.117.111385
This article has not been copyedited and formatted. The final version may differ from this version.

As for the regulation of ERα mRNA levels with test compounds, we employed qRT-PCR. The results demonstrate that E_2 down regulated the mRNA levels as soon as 6h of treatment though not statistically significantly (Fig. 6C). However, after 12 hours of treatment E_2 down regulated the mRNA levels by 50% compared to vehicle control ($p< 0.05$) and stayed consistently low for the rest of the time points (Fig. 6C). Interestingly, EtOXTPE down regulated the ERα mRNA expression only after 24 hours of treatment ($p< 0.05$ compared to vehicle control) (down by 50%) and even further down regulated the mRNA levels after 36h of treatment ($p< 0.05$ compared to vehicle control) (down by 60%) (Fig. 6C). ICI 182,780 (Fulvestrant) was used a positive control for ERα protein degradation in immunoblotting experiments (Fig. 6A & B) and as a negative control in qRT-PCR experiments (Fig. 6C). The results indicate that non-planar estrogen down regulates the ERα protein and mRNA levels as well as E_2 in MCF-7:5C cells, however, this effect was delayed over time.

Induction of unfolded protein response through PERK pathway by non-planar estrogen EtOXTPE in MCF-7:5C cells. One of the hallmarks and triggers of the estrogen-induced apoptosis in MCF-7:5C cells is the induction of unfolded protein response (UPR) at early time points of treatment with estrogens (Fan et al., 2013). Unfolded protein response initiates endoplasmic reticulum stress that activates PERK that subsequently activates eIF2α by phosphorylation (p-eIF2α). PERK pathway is essential for triggering estrogen-induced apoptosis. To assess the UPR through the phosphorylation of eIF2α we employed immunoblotting. Our results show that E_2 is able to induce phosphorylation of eIF2α as soon as 24h when compared to vehicle control (Fig. 6D), however, non-planar EtOXTPE increases levels of p-eIF2α equal to E_2 treatment only after 36h of treatment when compared to vehicle control (Fig. 6D). Additionally, antiestrogens endoxifen and ICI were used as negative controls and did not induce activation of

Molecular Pharmacology Fast Forward. Published on May 8, 2018 as DOI: 10.1124/mol.117.111385
This article has not been copyedited and formatted. The final version may differ from this version.

eIF2α and were able to reverse the E_2-induced and EtOXTPE-induced phosphorylation of eIF2α (Fig. 6D). Interestingly, EtOXTPE was able to reverse E_2-induced activation of eIF2α also, but only at 24 hours of treatment, and at later time points the both compounds induce the phosphorylation of eIF2α (Fig. 6D).

Recruitment of ERα and SRC3 on GREB1 promoter by non-planar estrogen EtOXTPE in MCF-7:5C cells. To assess and compare the effects of test compounds on the recruitment of ERα protein and SRC3 co-activator in MCF-7:5C cells we have employed Chromatin Immuno-Precipitation (ChIP) assay. We have done the ChIP assays after 45 minute and 36 hour time points. At the 45 minute time point of EtOXTPE recruits only 25% of ER to the GREB1 promoter compared with E_2 (Fig. 7A) and even less SRC3 after 45 minutes of treatment (Fig. 7B). After 36 hours of treatment EtOXTPE recruits about a half of ERα that E_2 does (Fig. 7C). Interestingly, 4OHT also has recruited as much ER as EtOXTPE after 36 hours of treatment (Fig. 7C), but after 45 minutes 4OHT recruited only twice as much as vehicle control (Fig. 7A) but no SRC3 is associated with the ER (Fig. 7B & D). EtOXTPE recruits very little of the SRC3 co-activator when compared to vehicle control at the 36 hour time point ($p>0.05$) and not more than 4OHT ($p>0.05$) (Fig. 7D). In summary, EtOXTPE behaves more like an antiestrogen in terms of co-activator recruitment to the estrogen responsive gene GREB1, however, biologically EtOXTPE is a partial agonist as demonstrated by growth assays and RT-PCR. This can indicate a different mechanism of ER activation for transcription based on a different surface conformation of the ER bound with the EtOXTPE compound.

Novel conformation of ERα LBD:EtOXTPE compared to estrogen, endoxifen, and 4OHT resolved by X-ray crystallography. To investigate the structural basis for EtOXTPE binding to the ERα ligand-binding domain (LBD) we obtained an x-ray crystal structure of the

Molecular Pharmacology Fast Forward. Published on May 8, 2018 as DOI: 10.1124/mol.117.111385
This article has not been copyedited and formatted. The final version may differ from this version.

co-crystallized complex. Clear density was observed in the ligand binding pocket corresponding to the trans-EtOXTPE isomer post-refinement (PBD code 5T1Z) (Fig. 8A). As such, this model shows that the trans isomer of EtOXTPE is preferred over the cis in the ERα LBD binding pocket. The ethoxy moiety is not well ordered in the map. This is likely due to the absence of any stabilizing interactions with the LBD making it free to adopt multiple conformations in the binding pocket. The EtOXTPE appears to mainly form non-polar interactions within the binding pocket. However, the hydrogen bond network formed between the A ring of estradiol, carboxylate group of E353, guanidinium group of R394 and a water molecule is conserved for the analogous phenol of EtOXTPE (Fig. 8A and 8B).

To investigate structural differences between the EtOXTPE structure and the planar estrogen E_2 an x-ray crystal structure of the ERα LBD Y537S mutant in complex with E_2 and GRIP peptide was solved to 1.65 Å using molecular replacement (PDB: 5DTA) (Fig. 8B). One dimer was observed in the asymmetric unit. Chain B of each structure was chosen for all comparisons because it is not influenced by crystal packing while Chain A shows crystal contacts at helices 11 and 12. Overall, both structures adopt the agonist conformation of the receptor with helix 12, shown in yellow in Fig. 8A and B, closing over the opening of the binding pocket. However, clear structural differences are apparent between the E_2 and EtOXTPE structures (Fig. 8A, 8B and Fig. S2 panel A). Notably, H524 is forced outside of the binding pocket by the bulkier phenol group of EtOXTPE and faces the solvent rather than adopting a conformation similar to that for E_2 (Fig. S2 panel A). Consequently, the formation of an H-bond with the ligand is no longer possible. In the ERα:E_2 complex, this H-bond is part of an extended H-bond network, starting at H524 side chain (helix 11) and terminating at E339 (helix 3) and K531 (helix 11) via E419. Thus, E_2 is arrested in the binding pocket and this network induces

Molecular Pharmacology Fast Forward. Published on May 8, 2018 as DOI: 10.1124/mol.117.111385
This article has not been copyedited and formatted. The final version may differ from this version.

stability to the E_2 agonist conformation of the receptor. This network in no longer formed in EtOXTPE structure and the receptor's stability is affected. The imidazole group of H524 forms H-bonds with the backbone of G521 and K520, while the amino group of K520 is involved in formation of a bridge salt with carboxylate group of E523 (Fig. S2 panel A). The side chains of L525 and L540 are shifted to accommodate and participate in Van Der Waals interactions with the ethoxybenzene group of EtOXTPE (Fig. 8A and Fig. S2 panel A). Together, these changes propagate to alter the vector of helix 11 such that it is now closer to helix 12 by 1.876 Å (Cα to Cα at C530) (Fig. S2 panel A). As a result, the carbonyl oxygen of Y526 breaks its hydrogen bond with the amide nitrogen of C530, placing the phi and psi angles of C530 outside the range for an alpha helix. Together, these structures show that EtOXTPE induces an alternative conformation of the ERα LBD compared to E_2.

EtOXTPE and endoxifen are structurally similar except that EtOXTPE is missing the terminal methylamine sidechain and additionally it has a phenolic hydroxyl group. Clear differences are observed between the x-ray crystal structures. Specifically, the bulkier terminal methylamine group of endoxifen forms hydrogen bonds with D351 and V533 (Fig. 8C) and forces helix 12 into the AF-2 cleft to block coregulator binding, similar to 4OHT structure (Fig. 8C8D, Fig. S2 panel B). The sum of the smaller size and absence of a hydrogen bond with D351 in the EtOXTPE arm, combined with its binding orientation which favors hydrophobic contacts with L536 and L540 of helix 12 enable the compound to stabilize the agonist conformation of the receptor (Fig. 8A), but to a lesser extent that E2. This conformation is not possible for endoxifen which, similarly to 4-OHT, contains a large ethoxyamino substituent that protrudes out of the binding pocket (Fig. 8D) and precludes the binding to the agonist conformation of ERα LBD,

Molecular Pharmacology Fast Forward. Published on May 8, 2018 as DOI: 10.1124/mol.117.111385
This article has not been copyedited and formatted. The final version may differ from this version.

due to steric clashes with helix 12, especially L536 and L540 (Fig. S2 panel C). All X-ray crystal structure data collection and refinement statistics are in Supplemental Table 4.

Discussion

An understanding of the modulation of estrogen-induced apoptosis through the ER has important implications for physiology through bone remodeling in osteoporosis and trophoblast turnover during implantation of the fertilized egg, in the prepared uterine lining (Jordan et al., 2016). These physiologic programs are also exposed during LTED therapy used to treat breast cancer (Jordan, 2015). We and others have previously reported (Lewis et al., 2005a; Lewis et al., 2005b; Song et al., 2001) that antiestrogen resistant breast cancer cells can trigger apoptosis with low dose estrogen treatment. This laboratory model has clinical significance as low and high dose estrogen has antitumor actions following LTED for breast cancer (Coelingh Bennink et al., 2017; Jordan, 2014a).

Here we address the hypothesis that a class II (angular) TPE derived estrogen (Jordan et al., 2001) has an initial antiestrogenic response at the LTED breast tumor cell ER (Maximov et al., 2011), but subsequently triggers apoptosis days later. We have observed that despite the slowed triggering of ER-mediated apoptosis by EtOXTPE, X-ray crystallographic studies demonstrate that helix 12 seals the ligand within the LBD similar to that observed with E_2 (Fig. 8). Nevertheless, the complex with EtOXTPE, referred to as 5T1Z, is distinct from the E_2 complex.

The delay in EtOXTPE-induced apoptosis is illustrated in Figure 2A and 2C and compared with endoxifen, an important antiestrogenic metabolite of tamoxifen (Jordan, 2017) recently reported to be effective for salvage therapy, following the failure of LTED therapy in breast cancer (Goetz et al., 2017). Endoxifen produces no apoptosis over the 14 day time course,

Molecular Pharmacology Fast Forward. Published on May 8, 2018 as DOI: 10.1124/mol.117.111385
This article has not been copyedited and formatted. The final version may differ from this version.

whereas EtOXTPE produced complete apoptosis within the same time period. The X-ray crystallography of endoxifen is reported for the first time and compared and contrasted with 4OHT and EtOXTPE (Fig. 8 and Fig. S1). Estradiol, the natural ER binding ligand, induces complete closure of the LBD (Fig. 8A) via helix 12 that facilitates binding of coactivators and the formation of the transcriptional complex (Fig. 7). It is important to note, however, that the initial biological response in the LTED breast cancer cells is growth stimulation with either E_2 or EtOXTPE (Fig. 2A). We have addressed this decision making mechanism to either grow or die in LTED breast cancer cells in an earlier publication (Fan et al., 2015). The interesting observation is that the class II estrogen EtOXTPE has a longer decision making mechanism (Fig. 2A & C).

EtOXTPE causes closure of the LBD with helix 12 locking the ligand inside, however, the complex is different than the E_2:ER complex, which may account for the rapidity of estradiol-induced apoptosis (Fig. 2C). Coactivator SRC3 was not rapidly recruited to the EtOXTPE complex (Fig. 7). Indeed, the fact that the EtOXTPE recruited ER and SRC3 to the TFF1 target gene promoter more like the antiestrogen 4OHT than E_2 provides an explanation for the delayed partial agonist actions of EtOXTPE at TFF1 and GREB1 (Fig. 7). Indeed, the related class II (angular) triphenylethylene bisphenol also has impaired recruitment of the ER to the TFF1 promoter (Sengupta et al., 2013) and 25% of SRC3 binding compared to E_2 or the planar Class I estrogen bisphenol A. This accounts for partial agonist actions at estrogen target genes in normal cell of the rat anterior pituitary gland (Jordan and Lieberman, 1984; Jordan et al., 1984) and MCF-7 breast cancer cells (Maximov et al., 2014; Obiorah et al., 2014; Sengupta et al., 2013).

Molecular Pharmacology Fast Forward. Published on May 8, 2018 as DOI: 10.1124/mol.117.111385
This article has not been copyedited and formatted. The final version may differ from this version.

Estrogen-induced apoptosis is the ultimate result of a protective mechanism embedded in the human genome to preserve fidelity of reproducing normal cells. The UPR response that triggers PERK signaling through eIF2α is delayed by EtOXTPE (fig. 6D). By contrast, apoptosis is not triggered by endoxifen (Fig. 2C) over a two week exposure. Additionally, apoptosis with EtOXTPE is rescued by addition of 4OHT within 48 hours after the addition of the estrogenic EtOXTPE (Fig. 2C). These data are consistent with previous results observed with the class II synthetic angular estrogen bisphenol (Obiorah and Jordan, 2014).

In summary, we provide the first studies to report the x-ray crystallography of the potent antiestrogenic metabolite endoxifen (Fig. 8C) and a class II angular estrogen EtOXTPE (Fig. 8A). Both have related structures based on the estrogen TPE (Fig. 1), but contrasting pharmacologic actions in the LTED cells MCF-7:5C; endoxifen does not induce apoptosis or trigger estrogen responsive gene transcription whereas EtOXTPE is a partial agonist but is unable to mobilize full agonist responses. Nevertheless, it is the relentless activation of the UPR sensor PERK that eventually initiates delayed apoptosis. The key to immediate efficient estrogen-induced apoptosis in LTED cells is the efficient recruitment of coregulators to the external surface of the TPE:ER complex. This mechanism has its origins in earlier work by the McDonnell group 20 years ago (Paige et al., 1999). A comparison of class II synthetic estrogens, apoptosis and coregulators recruitment, as previously reported by Han and coworkers (Han et al., 2016), will aid further understanding of the molecular modulation of estrogen-induced apoptosis via the ER.

These data illustrate the plasticity of the UPR system, that is dependent upon the shape of the ligand:ER complex to trigger apoptosis. However, it is the translation of these findings to clinical utility for patient care that holds the most promise. There is a concern that 5 years of

Molecular Pharmacology Fast Forward. Published on May 8, 2018 as DOI: 10.1124/mol.117.111385
This article has not been copyedited and formatted. The final version may differ from this version.

adjuvant therapy (Pan et al., 2017) is not sufficient to control disease recurrence for high-risk patients i.e.: large primary tumors and/or multiple lymph nodes. There is a proposal (Abderrahman and Jordan, 2018) to deploy estrogen-induced apoptosis and other precision medicines as a preemptive salvage therapy to lower micrometastatic tumor burden in high-risk patients. However, medicinal chemists have discovered (Xiong et al., 2016) raloxifene analogs that can occupy the ER LBD and trigger apoptosis without the collateral estrogenic activity. Studies are ongoing to address this hypothesis and a phase I trial is planned.

Authorship contributions

Participated in research design: P.Y. Maximov, V.C. Jordan

Conducted experiments: P. Y. Maximov, B. Abderrahman, S. Sengupta, P. Fan, D. M. Quintana Rincon, J. Greenland, S.W. Fanning, S. S. Rajan, G. L. Greene, R. F. Curpan

Performed data analysis: P. Y. Maximov, S.W. Fanning, R. F. Curpan, V. C. Jordan

Wrote or contributed to the writing of the manuscript: P. Y. Maximov, S. W. Fanning, R. F. Curpan, V. C. Jordan

Molecular Pharmacology Fast Forward. Published on May 8, 2018 as DOI: 10.1124/mol.117.111385
This article has not been copyedited and formatted. The final version may differ from this version.

References

Abderrahman B and Jordan VC (2016) The modulation of estrogen-induced apoptosis as an interpretation of the women's health initiative trials. *Exp Rev Endocrinol Metabol* **11:** 81-86.

Abderrahman B and Jordan VC (2018) Rethinking Extended Adjuvant Antiestrogen Therapy to Increase Survivorship in Breast Cancer. *JAMA Oncol* **4:** 15-16.

Coelingh Bennink HJ, Verhoeven C, Dutman AE and Thijssen J (2017) The use of high-dose estrogens for the treatment of breast cancer. *Maturitas* **95:** 11-23.

Cole MP, Jones CT and Todd ID (1971) A new anti-oestrogenic agent in late breast cancer. An early clinical appraisal of ICI46474. *Br J Cancer* **25:** 270-275.

EBCTCG (1998) Tamoxifen for early breast cancer: an overview of the randomised trials. Early Breast Cancer Trialists' Collaborative Group. *Lancet* **351:** 1451-1467.

Ellis MJ, Gao F, Dehdashti F, Jeffe DB, Marcom PK, Carey LA, Dickler MN, Silverman P, Fleming GF, Kommareddy A, et al. (2009) Lower-dose vs high-dose oral estradiol therapy of hormone receptor-positive, aromatase inhibitor-resistant advanced breast cancer: a phase 2 randomized study. *JAMA* **302:** 774-780.

Fan P, Agboke FA, Cunliffe HE, Ramos P and Jordan VC (2014a) A molecular model for the mechanism of acquired tamoxifen resistance in breast cancer. *Eur J Cancer* **50:** 2866-2876.

Fan P, Agboke FA, McDaniel RE, Sweeney EE, Zou X, Creswell K and Jordan VC (2014b) Inhibition of c-Src blocks oestrogen-induced apoptosis and restores oestrogen-stimulated growth in long-term oestrogen-deprived breast cancer cells. *Eur J Cancer* **50:** 457-468.

Fan P, Cunliffe HE, Griffith OL, Agboke FA, Ramos P, Gray JW and Jordan VC (2014c) Identification of gene regulation patterns underlying both oestrogen- and tamoxifen-stimulated cell growth through global gene expression profiling in breast cancer cells. *Eur J Cancer* **50:** 2877-2886.

Fan P, Cunliffe HE, Maximov PY, Agboke FA, McDaniel RE, Zou X, Ramos P, Russell ML and Jordan VC (2015) Integration of downstream signals of insulin-like growth factor-1 receptor by endoplasmic reticulum stress for estrogen-induced growth or apoptosis in breast cancer cells. *Mol Cancer Res* **13:** 1367-1376.

Fan P, Griffith OL, Agboke FA, Anur P, Zou X, McDaniel RE, Creswell K, Kim SH, Katzenellenbogen JA, Gray JW, et al. (2013) c-Src modulates estrogen-induced stress and apoptosis in estrogen-deprived breast cancer cells. *Cancer Res* **73:** 4510-4520.

Fanning SW, Mayne CG, Dharmarajan V, Carlson KE, Martin TA, Novick SJ, Toy W, Green B, Panchamukhi S, Katzenellenbogen BS, et al. (2016) Estrogen receptor alpha somatic mutations Y537S and D538G confer breast cancer endocrine resistance by stabilizing the activating function-2 binding conformation. *eLife* **5:** e12792.

Goetz MP, Suman VJ, Reid JM, Northfelt DW, Mahr MA, Ralya AT, Kuffel M, Buhrow SA, Safgren SL, McGovern RM, et al. (2017) First-in-human phase I study of the tamoxifen metabolite Z-endoxifen in women with endocrine-refractory metastatic breast cancer. *J Clin Oncol* 10.1200/JCO.2017.73.3246 JCO2017733246.

Gottardis MM and Jordan VC (1988) Development of tamoxifen-stimulated growth of MCF-7 tumors in athymic mice after long-term antiestrogen administration. *Cancer Res* **48:** 5183-5187.

Gottardis MM, Jiang SY, Jeng MH and Jordan VC (1989a) Inhibition of tamoxifen-stimulated growth of an MCF-7 tumor variant in athymic mice by novel steroidal antiestrogens. *Cancer Res* **49:** 4090-4093.

Gottardis MM, Wagner RJ, Borden EC and Jordan VC (1989b) Differential ability of antiestrogens to stimulate breast cancer cell (MCF-7) growth in vivo and in vitro. *Cancer Res* **49:** 4765-4769.

Haddow A (1970) David A. Karnofsky memorial lecture. Thoughts on chemical therapy. *Cancer* **26:** 737-754.

Haddow A, Watkinson JM, Paterson E and Koller PC (1944) Influence of Synthetic Oestrogens on Advanced Malignant Disease. *Br Med J* **2:** 393-398.

Han SJ, Begum K, Foulds CE, Hamilton RA, Bailey S, Malovannaya A, Chan D, Qin J and O'Malley BW (2016) The Dual Estrogen Receptor alpha Inhibitory Effects of the Tissue-Selective Estrogen Complex for Endometrial and Breast Safety. *Mol Pharmacol* **89:** 14-26.

Howell A, Robertson JF, Quaresma Albano J, Aschermannova A, Mauriac L, Kleeberg UR, Vergote I, Erikstein B, Webster A and Morris C (2002) Fulvestrant, formerly ICI 182,780, is as effective as anastrozole in postmenopausal women with advanced breast cancer progressing after prior endocrine treatment. *J Clin Oncol* **20:** 3396-3403.

Ingle JN, Ahmann DL, Green SJ, Edmonson JH, Bisel HF, Kvols LK, Nichols WC, Creagan ET, Hahn RG, Rubin J, et al. (1981) Randomized clinical trial of diethylstilbestrol versus tamoxifen in postmenopausal women with advanced breast cancer. *N Engl J Med* **304:** 16-21.

Jiang SY, Wolf DM, Yingling JM, Chang C and Jordan VC (1992) An estrogen receptor positive MCF-7 clone that is resistant to antiestrogens and estradiol. *Mol Cell Endocrinol* **90:** 77-86.

Jordan VC (2003) Tamoxifen: a most unlikely pioneering medicine. *Nat Rev Drug Discov* **2:** 205-213.

Jordan VC (2008) Tamoxifen: catalyst for the change to targeted therapy. *Eur J Cancer* **44:** 30-38.

Jordan VC (2014a) Linking estrogen-induced apoptosis with decreases in mortality following long-term adjuvant tamoxifen therapy. *J Natl Cancer Inst* **106:** dju296.

Jordan VC (2014b) Tamoxifen as the first targeted long-term adjuvant therapy for breast cancer. *Endocr Relat Cancer* **21:** R235-246.

Jordan VC (2015) The new biology of estrogen-induced apoptosis applied to treat and prevent breast cancer. *Endocr Relat Cancer* **22:** R1-31.

Jordan VC (2017) Endoxifen: the end, or are we at the beginning? *J Clin Oncol* 10.1200/JCO.2017.74.9325 JCO2017749325.

Jordan VC and Allen KE (1980) Evaluation of the antitumour activity of the non-steroidal antioestrogen monohydroxytamoxifen in the DMBA-induced rat mammary carcinoma model. *Eur J Cancer* **16:** 239-251.

Jordan VC, Dix CJ and Allen KE (1979) The effectiveness of long-term treatment in a laboratory model for adjuvant hormone therapy of breast cancer., in *Adjuvant therpy of cancer II*, (SE Salmon & SE Jones eds) pp 19-26, Greene and Stratton, New York.

Jordan VC, Fan P, Abderrahman B, Maximov PY, Hawsawi YM, Bhattacharya P and Pokharel N (2016) Sex steroid induced apoptosis as a rational strategy to treat anti-hormone resistant breast and prostate cancer. *Discov Med* **21:** 411-427.

Jordan VC and Lieberman ME (1984) Estrogen-stimulated prolactin synthesis in vitro. Classification of agonist, partial agonist, and antagonist actions based on structure. *Mol Pharmacol* **26:** 279-285.

Jordan VC, Lieberman ME, Cormier E, Koch R, Bagley JR and Ruenitz PC (1984) Structural requirements for the pharmacological activity of nonsteroidal antiestrogens in vitro. *Mol Pharmacol* **26:** 272-278.

Jordan VC, Schafer JM, Levenson AS, Liu H, Pease KM, Simons LA and Zapf JW (2001) Molecular classification of estrogens. *Cancer Res* **61:** 6619-6623.

Lewis JS, Meeke K, Osipo C, Ross EA, Kidawi N, Li T, Bell E, Chandel NS and Jordan VC (2005a) Intrinsic mechanism of estradiol-induced apoptosis in breast cancer cells resistant to estrogen deprivation. *J Natl Cancer Inst* **97:** 1746-1759.

Molecular Pharmacology Fast Forward. Published on May 8, 2018 as DOI: 10.1124/mol.117.111385
This article has not been copyedited and formatted. The final version may differ from this version.

Lewis JS, Osipo C, Meeke K and Jordan VC (2005b) Estrogen-induced apoptosis in a breast cancer model resistant to long-term estrogen withdrawal. *J Steroid Biochem Mol Biol* **94:** 131-141.

Maximov P, Sengupta S, Lewis-Wambi JS, Kim HR, Curpan RF and Jordan VC (2011) The Conformation of the Estrogen Receptor Directs Estrogen-Induced Apoptosis in Breast Cancer: A Hypothesis. *Horm Mol Biol Clin Investig* **5:** 27-34.

Maximov PY, Fernandes DJ, McDaniel RE, Myers CB, Curpan RF and Jordan VC (2014) Influence of the Length and Positioning of the Antiestrogenic Side Chain of Endoxifen and 4-Hydroxytamoxifen on Gene Activation and Growth of Estrogen Receptor Positive Cancer Cells. *J Med Chem* **57:** 4569-4583.

Maximov PY, Myers CB, Curpan RF, Lewis-Wambi JS and Jordan VC (2010) Structure-function relationships of estrogenic triphenylethylenes related to endoxifen and 4-hydroxytamoxifen. *J Med Chem* **53:** 3273-3283.

Moscetti L, Fabbri MA, Natoli C, Vici P, Gamucci T, Sperduti I, Iezzi L, Iattoni E, Pizzuti L, Roma C, et al. (2017) Fulvestrant 500 milligrams as endocrine therapy for endocrine sensitive advanced breast cancer patients in the real world: the Ful500 prospective observational trial. *Oncotarget* **8:** 54528-54536.

Nettles KW, Bruning JB, Gil G, Nowak J, Sharma SK, Hahm JB, Kulp K, Hochberg RB, Zhou H, Katzenellenbogen JA, et al. (2008) NFkappaB selectivity of estrogen receptor ligands revealed by comparative crystallographic analyses. *Nat Chem Biol* **4:** 241-247.

Obiorah I, Sengupta S, Curpan R and Jordan VC (2014) Defining the conformation of the estrogen receptor complex that controls estrogen-induced apoptosis in breast cancer. *Mol Pharmacol* **85:** 789-799.

Obiorah IE and Jordan VC (2014) Differences in the rate of oestrogen-induced apoptosis in breast cancer by oestradiol and the triphenylethylene bisphenol. *Br J Pharmacol* **171:** 4062-4072.

Osborne CK, Pippen J, Jones SE, Parker LM, Ellis M, Come S, Gertler SZ, May JT, Burton G, Dimery I, et al. (2002) Double-blind, randomized trial comparing the efficacy and tolerability of fulvestrant versus anastrozole in postmenopausal women with advanced breast cancer progressing on prior endocrine therapy: results of a North American trial. *J Clin Oncol* **20:** 3386-3395.

Paige LA, Christensen DJ, Gron H, Norris JD, Gottlin EB, Padilla KM, Chang CY, Ballas LM, Hamilton PT, McDonnell DP, et al. (1999) Estrogen receptor (ER) modulators each induce distinct conformational changes in ER alpha and ER beta. *Proc Natl Acad Sci U S A* **96:** 3999-4004.

Pan H, Gray R, Braybrooke J, Davies C, Taylor C, McGale P, Peto R, Pritchard KI, Bergh J, Dowsett M, et al. (2017) 20-Year Risks of Breast-Cancer Recurrence after Stopping Endocrine Therapy at 5 Years. *N Engl J Med* **377:** 1836-1846.

Sengupta S, Obiorah I, Maximov PY, Curpan R and Jordan VC (2013) Molecular mechanism of action of bisphenol and bisphenol A mediated by oestrogen receptor alpha in growth and apoptosis of breast cancer cells. *Br J Pharmacol* **169:** 167-178.

Sengupta S, Sharma CG and Jordan VC (2010) Estrogen regulation of X-box binding protein-1 and its role in estrogen induced growth of breast and endometrial cancer cells. *Horm Mol Biol Clin Investig* **2:** 235-243.

Song RX, Mor G, Naftolin F, McPherson RA, Song J, Zhang Z, Yue W, Wang J and Santen RJ (2001) Effect of long-term estrogen deprivation on apoptotic responses of breast cancer cells to 17beta-estradiol. *J Natl Cancer Inst* **93:** 1714-1723.

Xiong R, Patel HK, Gutgesell LM, Zhao J, Delgado-Rivera L, Pham TND, Zhao H, Carlson K, Martin T, Katzenellenbogen JA, et al. (2016) Selective Human Estrogen Receptor Partial Agonists (ShERPAs) for Tamoxifen-Resistant Breast Cancer. *J Med Chem* **59:** 219-237.

Yao K, Lee ES, Bentrem DJ, England G, Schafer JI, O'Regan RM and Jordan VC (2000) Antitumor action of physiological estradiol on tamoxifen-stimulated breast tumors grown in athymic mice. *Clin Cancer Res* **6:** 2028-2036.

Footnotes

This work was supported by the Department of Defense Breast Center of Excellence Program [W81XWH-06-1-0590]; the Susan G. Komen for the Cure Foundation [SAC100009]; the Lombardi Comprehensive Cancer Center Support Grant [NIH P30 CA051008]; the National Institutes of Health MD Anderson's Cancer Center Support Grant, [CA016672] and the Institute of Chemistry Timisoara of the Romanian Academy [Project no. 1.1/2015]; the Romanian National Authority for Scientific Research and Innovation, CNCS – UEFISCDI [PN-II-RU-TE-2014-4-0422]; the Department of Defense BCRP Breakthrough Award [W81XWH-14-1-0360]; the Susan G Komen Postdoctoral Fellowship [PDF14301382] and the Virginia and D. K. Ludwig Fund for Cancer Research.

Molecular Pharmacology Fast Forward. Published on May 8, 2018 as DOI: 10.1124/mol.117.111385
This article has not been copyedited and formatted. The final version may differ from this version.

Figure legends

Fig. 1 Chemical structures of compounds used in this study. EtOXPTE test compound is a 1:1 mixture or geometric isomers.

Fig. 2 Cell proliferation assays in MCF-7:5C antihormone resistant breast cancer cells. A: Effects of test compounds alone after 7 days of treatment. Results show that the only compound able to completely inhibit the growth of the cells is E_2, and the other test compounds possess no or only minor inhibitory effects; B: Antiestrogenic effects of test compounds in combination with 1nM E_2 after 7 days of treatment. Results show that all compounds exhibit antiestrogenic effects after 7 day treatment with the non-steroidal antiestrogens 4OHT and endoxifen completely inhibiting the effect of E_2 and angular estrogen EtOXTPE being able to inhibit E2 according to its intrinsic activity alone; C: Effects of test compounds alone on cells after 14 days of treatment. Results show that, besides E_2, EtOXTPE can inhibit the cell growth after 14 days of treatment. All non-steroid antiestrogenic compounds (4OHT, endoxifen) did not produce any inhibitory growth effect; D: Reversal of EtOXTPE-induced inhibitory effect on MCF-7:5C cells by 4OHT after pre-treatment of the cells with the test compound for various durations. All treatments were performed in triplicate, data represents average of the replicates.

Fig. 3 Bright field microscopy photographs of MCF-7:5C cell morphology after being treated with test compounds for indicated durations.

Fig. 4 A: Annexin V staining of MCF-7:5C cells after 3 days of treatment with 1nM E_2 and 6 days with EtOXTPE, 4OHT and endoxifen at 1μM concentrations; B: effects of 1μM EtOXTPE

Molecular Pharmacology Fast Forward. Published on May 8, 2018 as DOI: 10.1124/mol.117.111385
This article has not been copyedited and formatted. The final version may differ from this version.

on TNFα gene mRNA in MCF7:5C cells after 120 hours of treatment; C: effects of 1μM EtOXTPE on BCL2L11 gene mRNA in MCF7:5C cells after 120 hours of treatment; D: inhibition of EtOXTPE-induced apoptosis measured by Annexin V staining in MCF7:5C cells by PERK inhibitor. All treatments were performed in triplicate, data represents average of the replicates.

Fig. 5 Effects of well documented estrogen-responsive genes mRNA expression in MCF-7:5C cells after treatment with test compounds at different time points at 1nM concentration for E_2 and 1μM for other test compounds. A: TFF1 gene after 24 hours of treatment; B: GREB1 gene after 24 hours of treatment. All treatments were performed in triplicate, data represents average of the replicates.

Fig. 6 A: Effects of treatments with indicated compounds on ERα protein levels in MCF-7:5C cells after different durations of treatments at 1nM concentration for E_2 and 1μM for other test compounds; B: inhibition of ERα protein degradation induced by EtOXTPE and E_2 treatment after 36 hours of treatment in MCF-7:5C cells, E_2 was used at 1nM concentration and EtOXTPE was used at 100nM concentration, which is the minimum concentration at which the compound is able to still downregulate the ERα protein levels in the cells after 36 hours of treatment, 4OHT was used at 1uM concentration; C: Timecourse of treatments with indicated compounds and their effect on ERα mRNA gene expression in MCF-7:5C cells at 10nM concentration for E_2 and 1μM for other test compounds; C: reversal of ERα protein degradation by estrogens after a 48 hour treatment, including EtOXTPE at suboptimal concentration, by 1uM 4OHT; D: Levels if p-eIF2α after various duration of treatments with indicated compounds or their combinations. E_2 and

Molecular Pharmacology Fast Forward. Published on May 8, 2018 as DOI: 10.1124/mol.117.111385
This article has not been copyedited and formatted. The final version may differ from this version.

EtOXTPE both induce phosphorylation of eIF2α, however EtOXTPE has a delayed response. Antiestrogens, such as endoxifen and ICI do not induce phosphorylation of eIF2α at any time points, and inhibit activation of eIF2α by E_2 or EtOXTPE. At a 24 hour time point EtOXTPE acts as an antiestrogen and inhibits E_2-induced phosphorylation of eIF2α. In earlier work it was determined that PERK signaling protein in UPR was crucial for facilitating estrogen-induced apoptosis in MCF-7:5C cells via phosphorylation of eIF2α (Fan et al., 2013). All immunoblots were performed in three replicates, data presented represents one the biological replicates. Analysis was validated by densitometry using Image J (NIH) and the densitometry data is presented in supplemental tables S1, S2 and S3.

Fig. 7 ChIP assay showing recruitment of ERα and SRC3 at TFF1 ERE promoter after treatment (45 minutes and 36 hours) with test compounds in MCF7:5C cells at 10nM concentration for E_2 and 1μM for other test compounds. A: The recruitment of ERα and B: SRC3 after 45 minutes of treatment with indicated ligands. C: The recruitment of ERα and D: SRC3 after 36 hours of treatment with indicated ligands. Recruitment of ERα and SRC3 was calculated as percent of the total input after subtracting the IgG recruitment. All treatments were performed in triplicate, data represents average of the replicates.

Fig. 8 Overall structures and close-up views of the binding site of ERα LBD in complex with EtOXTPE (A), E2 (B), endoxifen (C) and 4OHT (D). On the left side of each panel is shown the overall structure of ERα LBD in complex with the ligands represented as spheres with helix 12 depicted in yellow, AF-2 site colored in blue and co-activator proteins in the agonist conformations (A, B) shown in green. On the right side is presented a close-up view of the

Molecular Pharmacology Fast Forward. Published on May 8, 2018 as DOI: 10.1124/mol.117.111385
This article has not been copyedited and formatted. The final version may differ from this version.

binding site of ERα LBD displaying the ligands and aminoacids involved in the formation of H-bonds and hydrophobic contacts. H-bonds are depicted as blue dashed lines.

Molecular Pharmacology Fast Forward. Published on May 8, 2018 as DOI: 10.1124/mol.117.111385
This article has not been copyedited and formatted. The final version may differ from this version.

Fig. 1

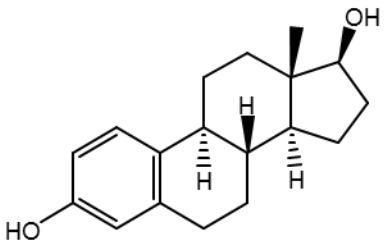

17β-estradiol (E_2)
(Class I planar estrogen)

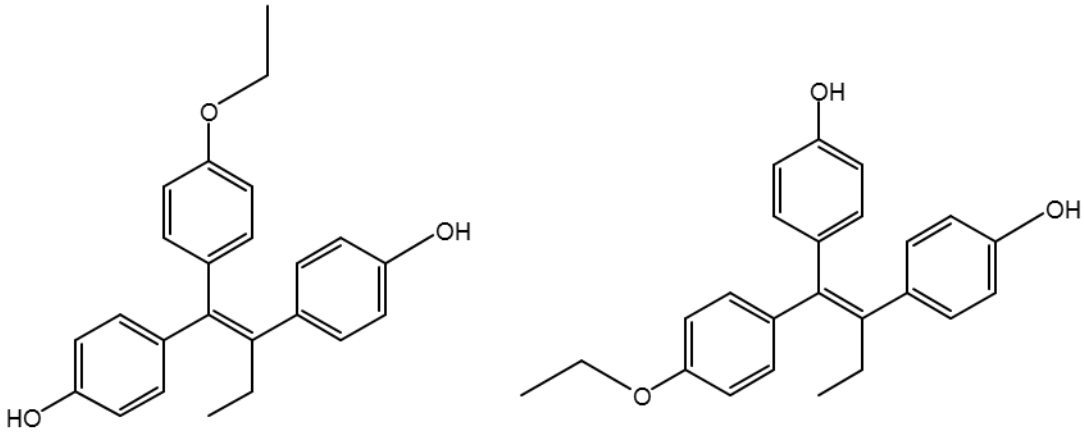

isomeric mixture of ethoxytriphenylethylene (EtOXTPE)
(classII angular estrogen)

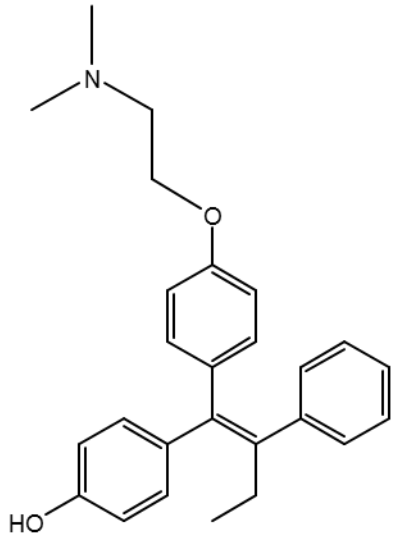

Z-4-hydroxytamoxifen (4OHT)
(non-steroidal antiestrogen)

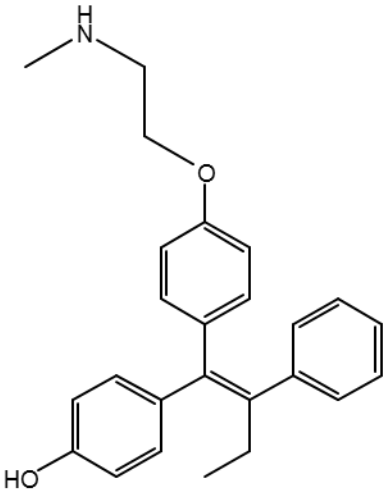

Endoxifen
(non-steroidal antiestrogen)

Molecular Pharmacology Fast Forward. Published on May 8, 2018 as DOI: 10.1124/mol.117.111385
This article has not been copyedited and formatted. The final version may differ from this version.

Fig. 2

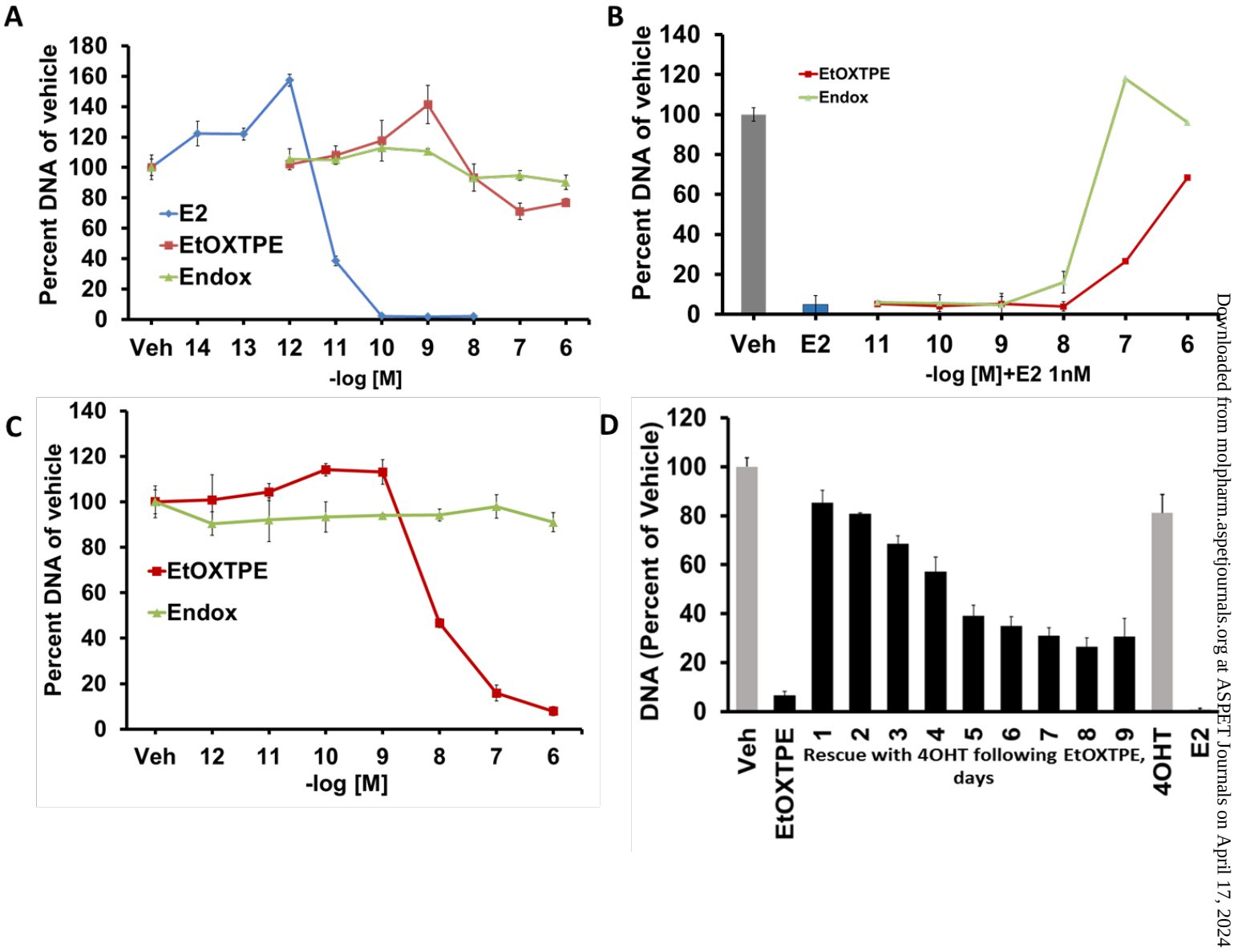

Molecular Pharmacology Fast Forward. Published on May 8, 2018 as DOI: 10.1124/mol.117.111385
This article has not been copyedited and formatted. The final version may differ from this version.

Fig. 3

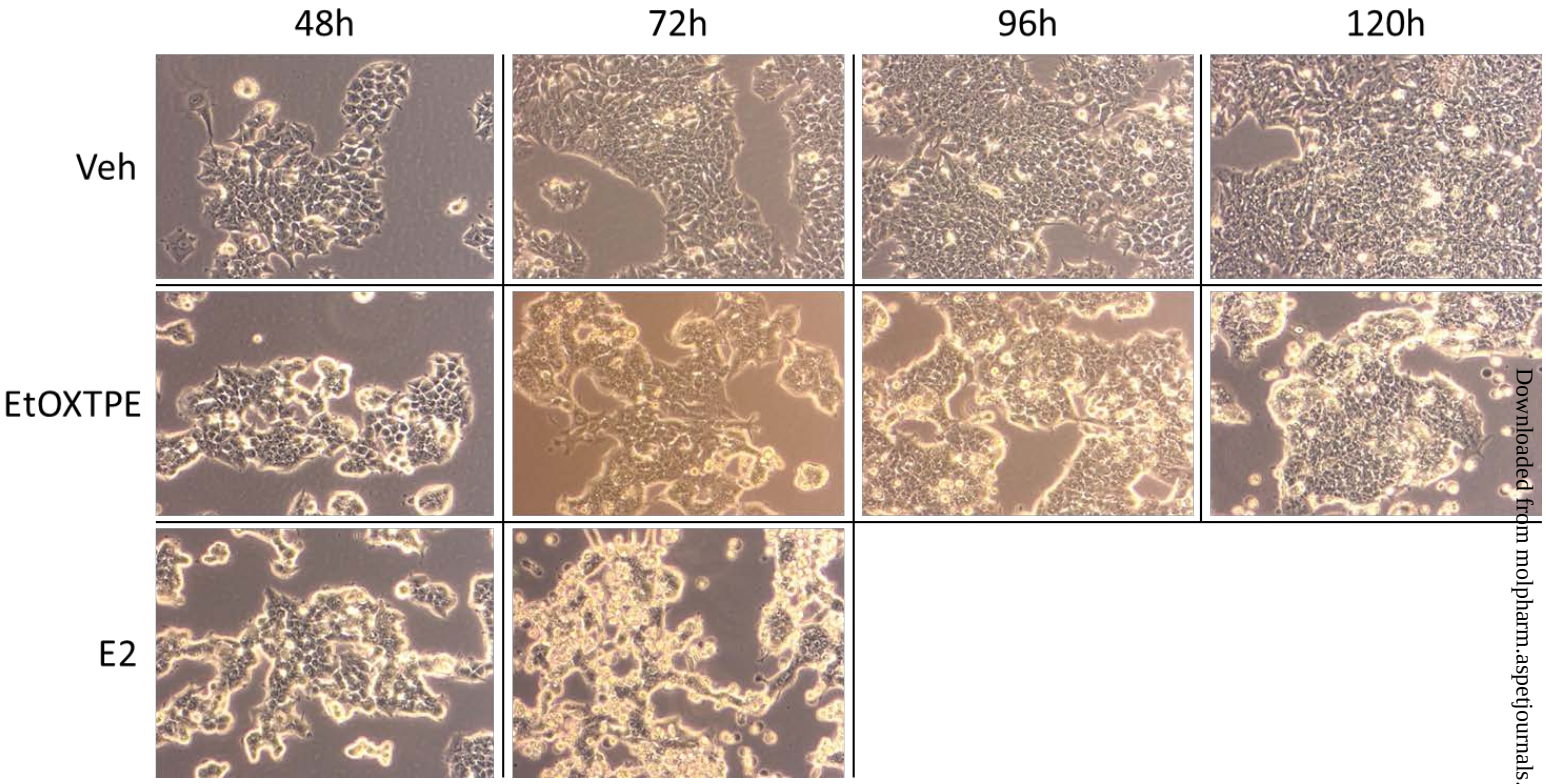

Molecular Pharmacology Fast Forward. Published on May 8, 2018 as DOI: 10.1124/mol.117.111385
This article has not been copyedited and formatted. The final version may differ from this version.

Fig. 4

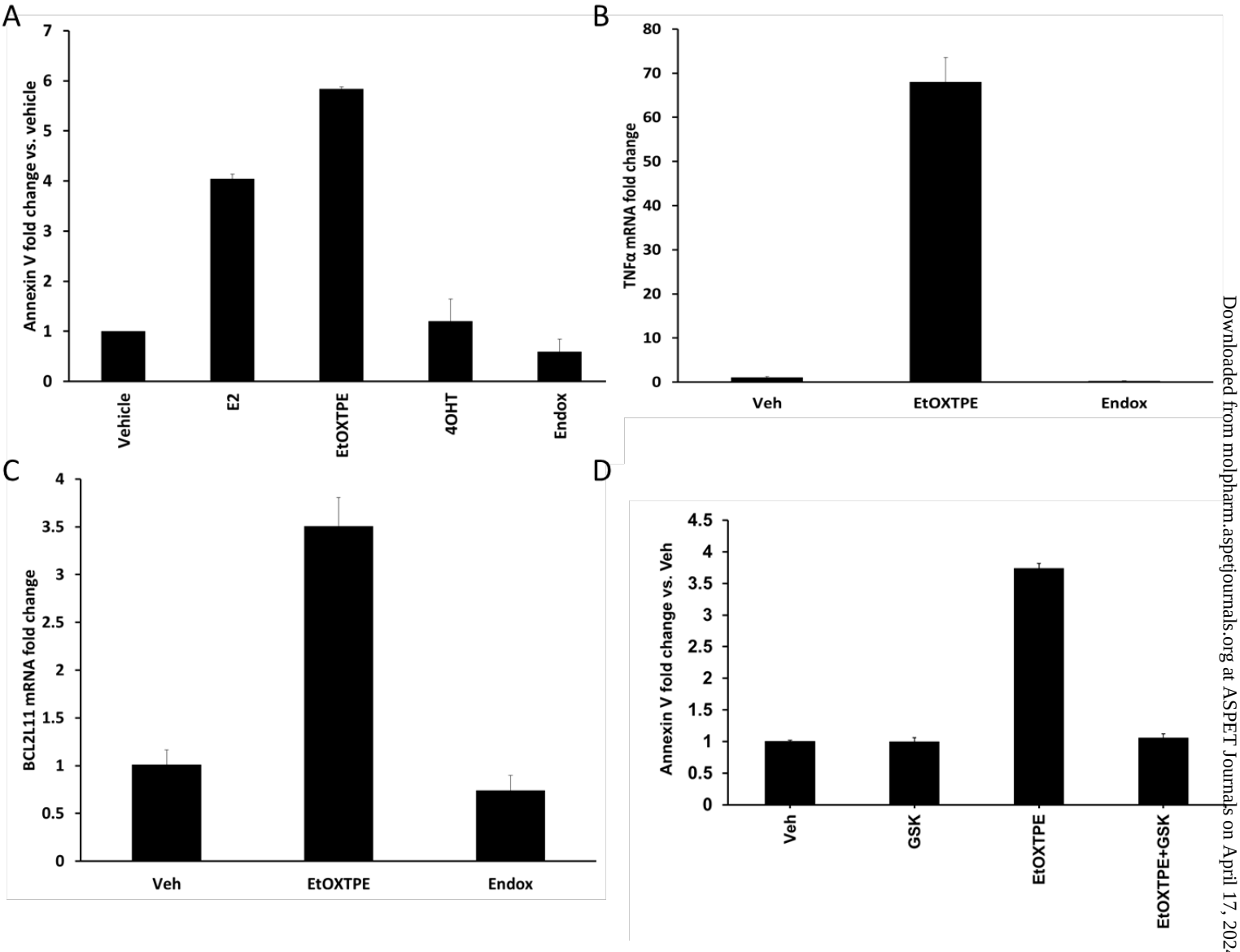

Molecular Pharmacology Fast Forward. Published on May 8, 2018 as DOI: 10.1124/mol.117.111385
This article has not been copyedited and formatted. The final version may differ from this version.

Fig. 5

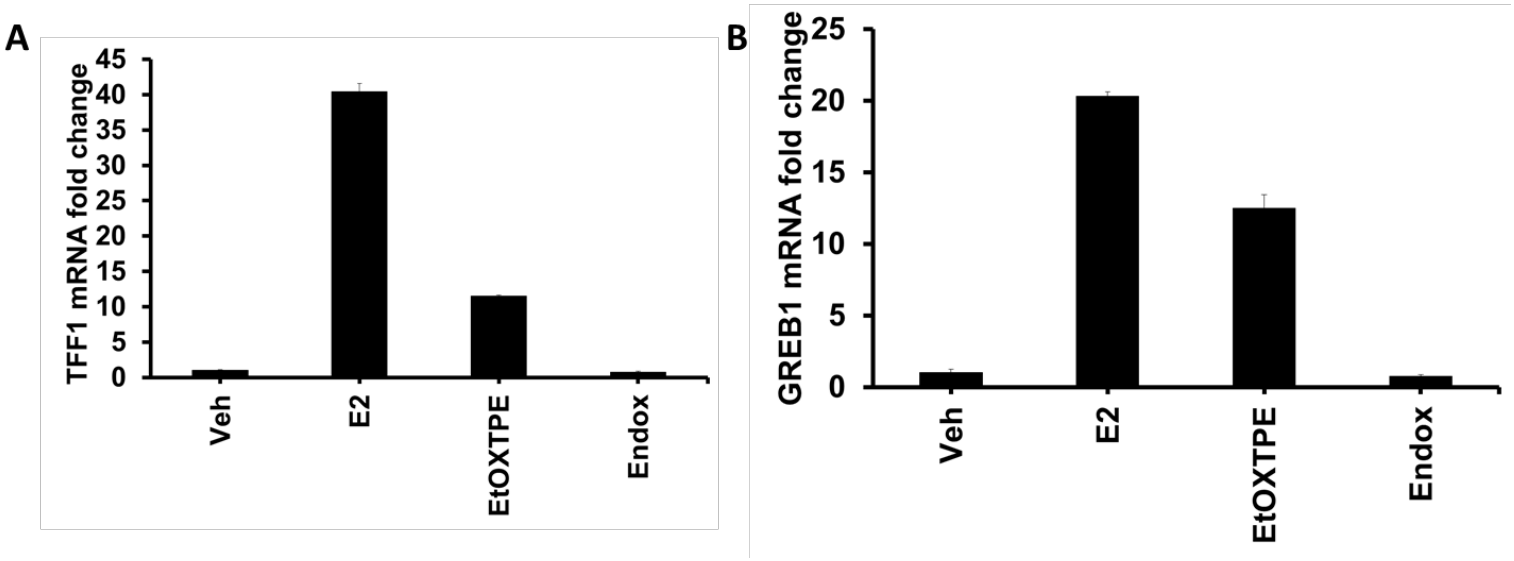

Molecular Pharmacology Fast Forward. Published on May 8, 2018 as DOI: 10.1124/mol.117.111385
This article has not been copyedited and formatted. The final version may differ from this version.

Fig. 6

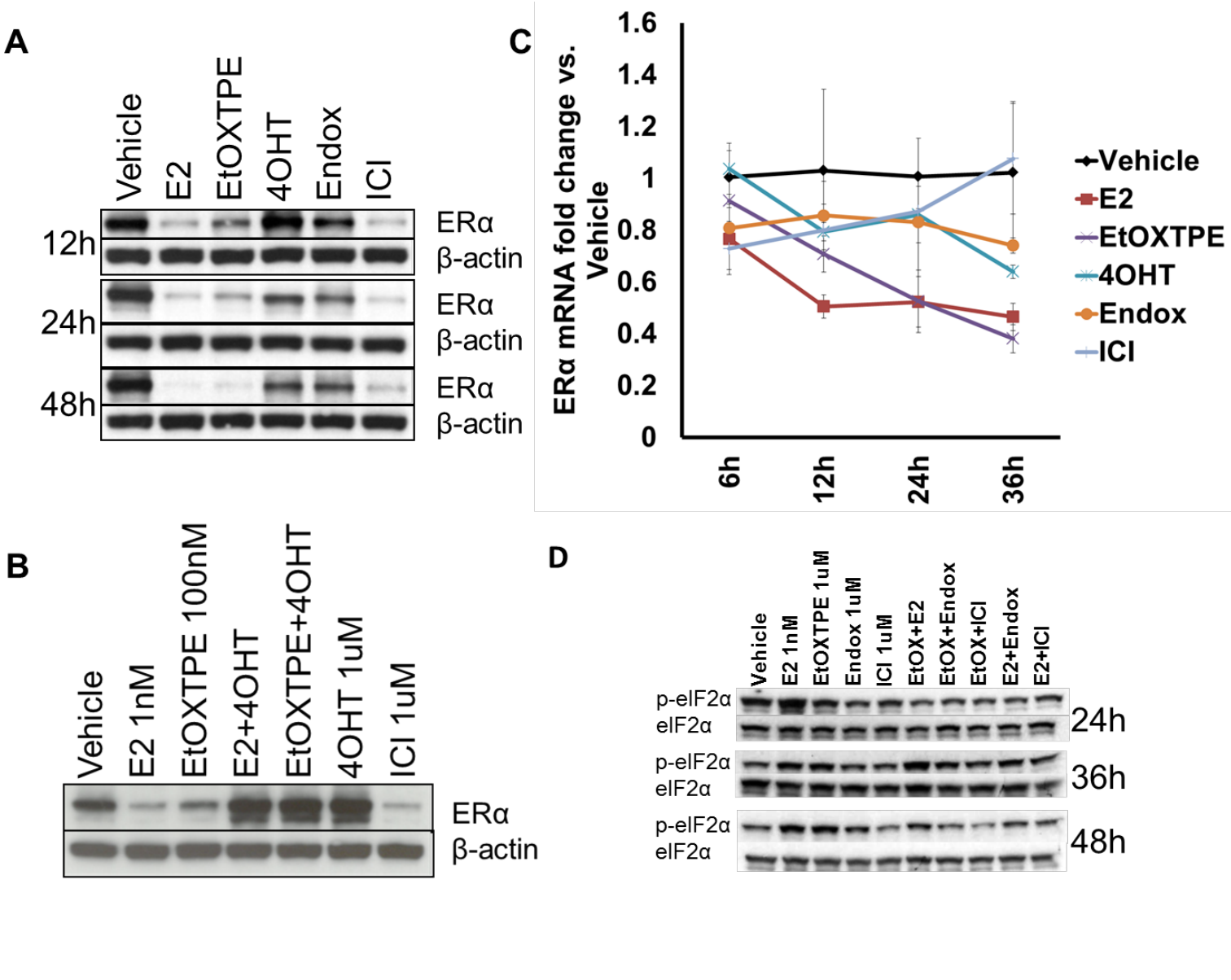

Molecular Pharmacology Fast Forward. Published on May 8, 2018 as DOI: 10.1124/mol.117.111385
This article has not been copyedited and formatted. The final version may differ from this version.

Fig. 7

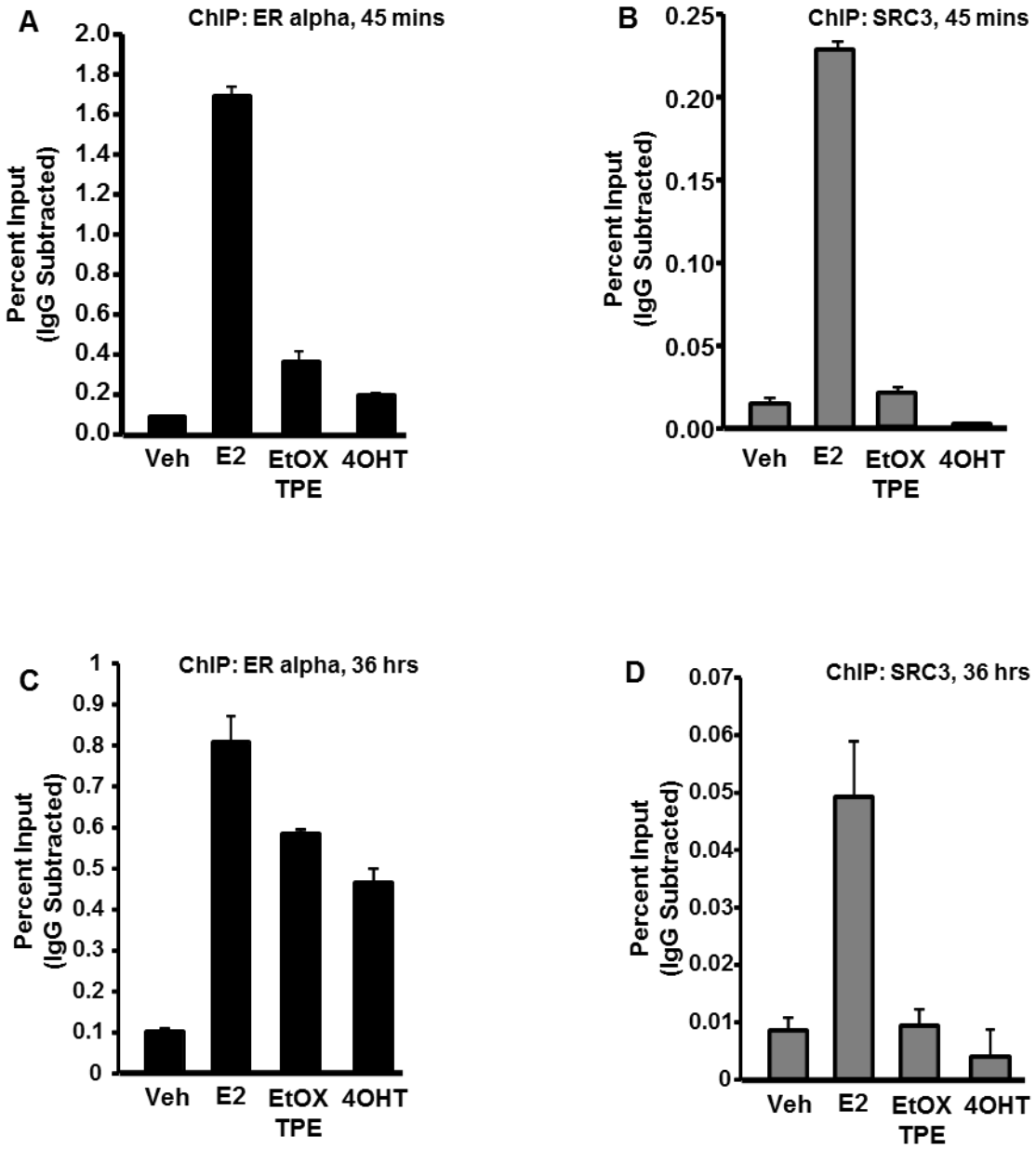

Molecular Pharmacology Fast Forward. Published on May 8, 2018 as DOI: 10.1124/mol.117.111385
This article has not been copyedited and formatted. The final version may differ from this version.

Fig. 8